STAT5 Induces Macrophage Differentiation of M1 Leukemia Cells Through Activation of IL-6 Production Mediated by NF-κB p65[1]

Toshiyuki Kawashima,*§ Ken Murata,* Shizuo Akira,‡ Yukio Tonozuka,* Yukinori Minoshima,* Sizhou Feng,* Hidetoshi Kumagai,* Hiromichi Tsuruga,* Yasuo Ikeda,§ Shigetaka Asano,† Tetsuya Nosaka,* and Toshio Kitamura[2]*

We recently demonstrated that STAT5 can induce a variety of biological functions in mouse IL-3-dependent Ba/F3 cells; STAT5-induced expression of *pim-1*, p21$^{WAF/Cip1}$, and *suppressor of cytokine signaling-1/STAT-induced STAT inhibitor-1/Janus kinase binding protein* is responsible for induction of proliferation, differentiation, and apoptosis, respectively. In the present study, using a constitutively active STAT5A (STAT5A1*6), we show that STAT5 induces macrophage differentiation of mouse leukemic M1 cells through a distinct mechanism, autocrine production of IL-6. The supernatant of STAT5A1*6-transduced cells contained sufficient concentrations of IL-6 to induce macrophage differentiation of parental M1 cells, and STAT3 was phosphorylated on their tyrosine residues in these cells. Treatment of the cells with anti-IL-6 blocking Abs profoundly inhibited the differentiation. We also found that the STAT5A1*6 transactivated the IL-6 promoter, which was mediated by the enhanced binding of NF-κB p65 (RelA) to the promoter region of IL-6. These findings indicate that STAT5A cooperates with Rel/NF-κB to induce production of IL-6, thereby inducing macrophage differentiation of M1 cells in an autocrine manner. In summary, we have shown a novel mechanism by which STAT5 induces its pleiotropic functions. Cytokines *The Journal of Immunology*, **2001, 167: 3652–3660.**

The STAT family is known to consist of seven members (STAT1–4, 5A, 5B, and 6), with STAT5A and STAT5B being closely related. STATs are activated by tyrosine phosphorylation, form homo- or heterodimers, and translocate into the nucleus, where they regulate expression of their target genes. STAT5, which was originally identified as a mammary gland factor regulated by prolactin (1), is activated by multiple cytokines including IL-2, IL-3, IL-5, GM-CSF, erythropoietin (EPO),[3] and thrombopoietin (2–7). We recently identified constitutively active mutants of STAT5 (STAT5A1*6 and STAT5A-N642H) by PCR-driven random mutagenesis and retrovirus-mediated expression screening (8, 9). A molecular basis for the constitutive activity of these mutants is the stability of the phosphorylated molecule. Using these constitutively active forms of STAT5, we found that activation of STAT5 induced cytokine-independent growth of IL-3-dependent cells (8, 9), and that STAT5 manifested a variety of biological functions including proliferation, differentiation, and apoptosis of Ba/F3 cells through up-regulation of a variety of target genes of STAT5 (10). In the present study, we attempted to determine the function of STAT5A in macrophage differentiation using a constitutively active STAT5A, STAT5A1*6, which has two mutations; one in the DNA binding domain (H298R) and the other in the transactivation domain (S710F) (8).

A myeloblastic leukemia cell line, M1, was generated from a spontaneous leukemia that arose within the SL strain of mice (11) and can be induced to undergo terminal differentiation into macrophages, which is associated with growth arrest and apoptosis of mature cells (12) by IL-6, LIF, or human oncostatin M (OSM) (13–15). Ectopic expression of the α and β subunits of the human GM-CSF receptor in M1 cells confers a potential to terminally differentiate into macrophages upon stimulation with human GM-CSF (16). Because STAT5 is one of the key molecules that are activated in response to GM-CSF (6, 17), we asked whether STAT5 is involved in monocytic differentiation of M1 cells. STAT5A1*6 induced macrophage differentiation of M1 cells, but through an unexpected mechanism. Activation of STAT5 leads to IL-6 production following enhancement of the DNA binding activity of NF-κB p65, suggesting a potential role of STAT5A to regulate IL-6-induced hemopoietic cell differentiation within the myelomonocytic lineage.

Materials and Methods

Culture, cytokines, and Abs

The murine myeloid leukemia cell line M1 was grown in DMEM (Life Technologies, Rockville, MD) containing 10% FCS. Mouse (m)IL-3-dependent Ba/F3 cells were maintained in RPMI 1640 medium containing 10% FCS and 1 ng/ml rmIL-3 produced in silk worm (18). An ecotropic retrovirus packaging cell line BOSC23 (19) was maintained in DMEM containing 10% FCS and guanine phosphoribosyltransferase selection reagents (Specialty Media, Lavallette, NJ). The cells were transferred into DMEM containing 10% FCS, without guanine phosphoribosyltransferase selection reagents, 2 days before transfection. The mIL-6, goat anti-mIL-6 neutralizing Ab (anti-IL-6 Ab), and goat anti-mLIF neutralizing Ab (anti-

*Division of Hematopoietic Factors and †Department of Hematology/Oncology, Institute of Medical Science, University of Tokyo, Tokyo, Japan; ‡Department of Host Defense, Core Research for Engineering, Science, and Technology of Japan Science and Technology Corporation, Research Institute for Microbial Diseases, Osaka University, Suita, Japan; and §Division of Hematology, Department of Internal Medicine, School of Medicine, Keio University, Tokyo, Japan

Received for publication November 14, 2000. Accepted for publication July 19, 2001.

The costs of publication of this article were defrayed in part by the payment of page charges. This article must therefore be hereby marked *advertisement* in accordance with 18 U.S.C. Section 1734 solely to indicate this fact.

[1] This work was supported by grants from the Ministry of Education, Science, Sports, and Culture; the Ministry of Health and Welfare, Japan; and CLONTECH Japan. The division of Hematopoietic Factors is supported by the Chugai Pharmaceutical.

[2] Address correspondence and reprint requests to Dr. Toshio Kitamura, Division of Hematopoietic Factors, Institute of Medical Science, University of Tokyo, 4-6-1 Shirokanedai, Minato-ku, Tokyo 108-8639, Japan. E-mail: kitamura@ims.u-tokyo.ac.jp

[3] Abbreviations used in this paper: EPO, erythropoitin; OSM, oncostatin M; m, mouse; EGFP, enhanced green fluorescent protein; IRES, internal ribosomal entry site; FSC, forward scatter; SSC, side scatter.

 0022-1767/01/$02.00

LIF Ab) were obtained from R&D Systems (Minneapolis, MN). PE-conjugated rat anti-mouse CD14 Ab were purchased from BD PharMingen (San Diego, CA).

Retrovirus vectors

A bicistronic retrovirus vector pMX-IRES-EGFP was constructed to transduce a gene together with an enhanced green fluorescent protein (EGFP) as previously described (10). Complementary DNAs for the wild-type mSTAT5A and STAT5A1*6 were inserted into *Eco*RI and *Not*I sites of the pMX-IRES-EGFP to construct pMX-STAT5A-IRES-EGFP and pMX-STAT5A1*6-IRES-EGFP.

Production of retroviruses and infection with these viruses

High-titer retroviruses containing the wild-type STAT5A and STAT5A1*6 were produced in a transient retrovirus packaging cell line BOSC23 as previously described (20). For infection, M1 cells (1×10^6) were incubated for 6 h with 10 ml of the retroviruses harboring the wild-type and STAT5A1*6 in the presence of 10 μg/ml hexadimethrine bromide (Sigma, St. Louis, MO). Ten milliliters of fresh growth medium was added to the culture, and incubation was continued for 18 h. The cells were washed, refed with growth medium, and allowed to grow for 1 more day before cell sorting.

Cell sorting and flow cytometry

Sorting of EGFP-positive cells was done as previously described (21). Briefly, 2 days after virus infection, cells were washed twice with PBS and suspended in PBS containing 1% BSA. Retrovirally transduced cells were sorted based on GFP expression on a FACSVantage (BD Biosciences, Mountain View, CA). The sorted cells (1×10^4) were washed twice with PBS, resuspend in growth medium, and cultured for 2 more days (4 days after virus infection). A half of the sorted population was used to confirm GFP expression using FACSCalibur (BD Biosciences), and the other half was expanded and used for further analysis.

Immunoprecipitation and Western blotting

Immunoprecipitation, gel electrophoresis, and immunoblotting were done as previously described (10) with minor modifications. Exponentially growing cells were washed in PBS so as to be free of serum and growth factors, lysed in a buffer (5×10^6 cells/ml), and incubated on ice for 30 min. Cell lysates were clarified by centrifugation for 15 min at 12,000 $\times$ *g* before incubation at 4°C overnight with the anti-STAT5A polyclonal Ab (R&D Systems) or the control rabbit whole IgG, and protein A-Sepharose. The immunoprecipitates were washed three times with a lysis buffer, subjected to SDS-PAGE, and electrophoretically transferred onto Immobilon filters (Millipore, Bedford, MA). After blocking in a solution containing 3% BSA, the filter was probed with an anti-phosphotyrosine Ab 4G10 (Upstate Biotechnology, Lake Placid, NY), stripped, and reprobed with the anti-STAT5A Ab to verify the amount loaded. The filter-bound Ab was detected using the ECL system (Amersham, Arlington Heights, IL).

EMSA in M1 cells

The cells were lysed in a binding buffer (2×10^7 cells/ml) containing 0.5% Nonidet P-40, 50 mM Tris-HCl (pH 8.0), 0.1 mM EDTA, 150 mM NaCl, 100 μM Na_3VO_4, 50 mM NaF, 1 mM DTT, 0.4 mM PMSF, 3 μg/ml aprotinin, 2 μg/ml pepstatin A, 1 μg/ml leupeptin, and 10% glycerol and were centrifuged at 12,000 $\times$ *g* for 30 min to remove insoluble materials. The cell extracts (4 μl/each reaction) were incubated with 1 ng of Klenow-labeled DNA carrying the following STAT5 optimal binding sequence: 5′-GATCCGAATTCCAGGAATTCA-3′ and 3′-GCTTAAGGTCCTTA AGTCTAG-5′. For supershift analysis, cell extract in the binding buffer was incubated with the anti-STAT5A rabbit anti-serum (R&D Systems) or normal rabbit serum, as a control, for 30 min on ice before addition of poly(dI-dC). Samples were separated on a 4.5% polyacrylamide gel in 2.2× TBE (1× TBE = 50 mM Tris-borate and 1 mM EDTA) and autoradiographed.

Luciferase reporter assay

Ba/F3 cells were transiently transfected by electroporation at 960 μF and 300 V with 10 μg of a reporter plasmid carrying a luciferase gene driven by the IL-6 promoter, 3 μg of a β-galactosidase reporter plasmid with the Rous sarcoma virus long-terminal repeat promoter, and 10 μg of test DNAs at room temperature in RPMI 1640 supplemented with 10 μg/ml DEAE-dextran. After a 12-h recovery period in the IL-3-containing medium, cells were incubated in RPMI 1640 supplemented with 0.5% BSA for 12 h, or stimulated with 2 ng/ml mIL-3 for the last 6 h before cell lysates were prepared. Cell lysates were then subjected to luciferase (Promega, Madison, WI) and β-galactosidase (Stratagene, La Jolla, CA) assays. Transfection efficiency was normalized with the β-galactosidase activity. The wild-type IL-6 promoter (k0) and its deletion mutants (k4, k18, and k9) were as previously described (22). Site-directed mutagenesis of k0 and k9 was done using QuikChange (Stratagene) and the oligonucleotide primers 5′-ATCAAATGTAATATTTTCCCATGAGTCTGA-3′ and 5′-TGAGACTCATGGGAAAATATTACATTTGAT-3′.

Transfection and preparation of nuclear extracts in COS cells

Cells were cotransfected with 1 μg of human Epo receptor gene, 1 μg pEF-NF-κB p65, and 1 μg of either pMX, pMX/WT-STAT5A, or pMX/STAT5A1*6 using FuGENE 6 Transfection Reagent (Roche Diagnostics, Indianapolis, IN). Forty-eight hours after transfection, cells were stimulated with recombinant human Epo (20 U/ml) for 30 min or left untreated before harvesting. Nuclear extracts were then prepared as previously described (10).

EMSA in COS, M1, and MD cells

Double-stranded oligonucleotides corresponding to the NF-κB site of the IL-6 promoter were used as DNA probes. EMSA was done using 10 μg of nuclear extracts in 25 μl of a reaction mixture containing 10 mM HEPES (pH7.8), 4% glycerol, 0.02 mM EDTA, 84 mM KCl, 1 mM $MgCl_2$, 3 μg of poly(dI-dC), 5 mM DTT, and 10 fmol of radioactive probe. The mixture was incubated on ice for 20 min and placed onto a 4.5% polyacrylamide gel (0.25× TAE). For supershift experiments, 1 μl of anti-NF-κB p65 Ab, anti-c-Rel Ab (Santa Cruz Biotechnology, Santa Cruz, CA), control rabbit polyclonal IgG, or anti-STAT5A Ab (R&D Systems) was added to the mixture.

Results

*The constitutively active mutant of STAT5A (STAT5A1*6) induced monocytic differentiation of M1 myeloid leukemic cells*

To elucidate the role of STAT5A in macrophage differentiation of M1 cells, the wild-type STAT5A and the constitutively active mutant STAT5A1*6 were transduced into M1 cells using a bicistronic retrovirus vector, pMX-IRES-EGFP, and a retrovirus packaging cell line, BOSC23 (19). EGFP-positive M1 cells transduced with pMX-STAT5A-IRES-EGFP and pMX-STAT5A1*6-IRES-EGFP were sorted on FACS 48 h after virus infection, as previously described (21), and were termed M1/WT-STAT5A and M1/STAT5A1*6, respectively. With May-Grünwald-Giemsa staining of cytospin preparations, the sorted M1/WT-STAT5A and M1/STAT5A1*6 cells exhibited the typical blast morphology of the parental M1 cells until 4 days after virus infection (data not shown). In flow cytometric analysis, both transfectants displayed little phenotypic change within 4 days, although both expressed a high level of EGFP (Fig. 1*A*). However, 7 days after the virus infection, some of M1/STAT5A1*6 became enlarged, and at 2 wk after the infection, M1/STAT5A1*6 cells exhibited a mixed pattern of morphology in culture, with both nonadherent and adherent cells. Microscopic examination of the M1/WT-STAT5A and the M1/STAT5A1*6 cells following May-Grünwald-Giemsa staining showed that STAT5A1*6, but not the wild-type STAT5A, induced M1 cells to differentiate into various stages along the monocytic differentiation pathway, giving rise to a heterogeneous population of blast, intermediate, and mature monocytic stages (Fig. 1*B*). Flow cytometric analysis was also done to quantitate the morphological changes in the M1/WT-STAT5A and the M1/STAT5A1*6 cells. The increase in size and granulosity of the cytoplasm, a hallmark of monocytic differentiation, observed in M1/STAT5A1* 6 cells was evaluated by forward scatter (FSC) and side scatter (SSC), respectively (Fig. 1*C*, *upper panels*), and 66.4% of M1/STAT5A1*6 cells showed a shift from region R1 to region R2 with increased size and granulosity. This shift pattern is similar to that of parental M1 cells cultured in the presence of IL-6 (100 ng/ml) for 5 days (data not shown). In addition, most of M1/

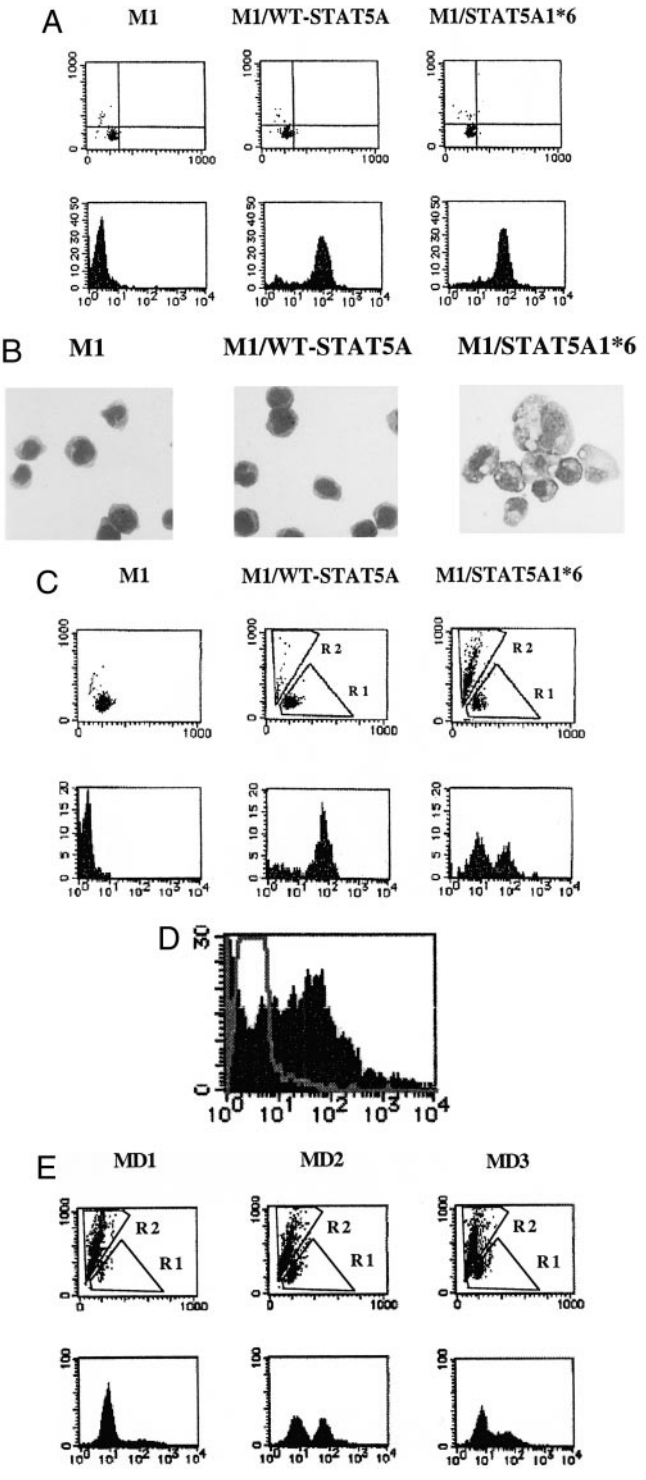

FIGURE 1. Macrophage differentiation of M1 cells transduced with pMX-IRES-EGFP-STAT5A1*6 (M1/STAT5A1*6). *A*, Quantitation of cell differentiation and expression of GFP 4 days after retroviral gene transduction (2 days after cell sorting) on flow cytometry in M1/WT-STAT5A and M1/STAT5A1*6 cells. *Upper panels*, The *x*-axis indicates FSC, and the *y*-axis indicates SSC. *Lower panels*, The *x*-axis indicates fluorescence intensity as a log scale ranging from 10^0 to 10^4, and the *y*-axis indicates the number of cells. Parental M1 cells were used as a control. *B*, Morphological analysis of STAT5A1*6-induced differentiation of M1 cells 10 days after gene transduction. Parental M1, M1/WT-STAT5A, and M1/STAT5A1*6 cells were centrifuged onto glass slides and stained with May-Grünwald-Giemsa. Photographs were taken at ×400 magnification. *C*, Flow cytometric analysis in parental M1, M1/WT-STAT5A, and M1/STAT5A1*6 cells 10 days after gene transduction. *Upper panels*, Quantitation of cell differentiation on flow cytometry. Differentiated M1 cells were detected in region R2. Increased size and vacuolization of differentiated cells are reflected by increases in FSC (*x*-axis) and SSC (*y*-axis), respectively. *Lower panels*, Quantitation of expression of GFP on flow cytometry. The *x*-axis indicates fluorescence intensity as a log scale ranging from 10^0 to 10^4. The *y*-axis indicates the number of the cells. *D*, CD14 expression of M1/WT-STAT5A and M1/STAT5A1*6 cells. M1/WT-STAT5A (blank area) and M1/STAT5A1*6 (shaded area) cells were preincubated with an isotype control rat IgG1 and stained with PE-conjugated rat anti-mouse CD14 Ab. The *x*-axis indicates fluorescence intensity as a log scale ranging from 10^0 to 10^4. The *y*-axis indicates the number of the cells. *E*, Quantitation of M1 cell differentiation on FACS in continuously growing clones, MD1, MD2 and MD3, derived from M1/STAT5A1*6 cells. The *x*-axis indicates FSC, and the *y*-axis indicates SSC.

STAT5A1*6 cells exhibited de novo expression of a myelomonocytic marker CD14 (Fig. 1*D*). IL-6, LIF, and human OSM induce terminal differentiation of the parental M1 cells into macrophages and eventuate cell death (13–15). In contrast, M1/STAT5A1*6 cells underwent monocytic differentiation, with a proliferating population retaining blastic phenotypes. Three such clones were isolated by limiting dilution and were termed MD1, MD2, and MD3 (M1 cells undergoing monocytic differentiation with expression of the STAT5A1*6). Flow cytometric analysis of these clones revealed basically similar phenotypes (Fig. 1*E*). They continuously proliferated, retaining a population of blast (region R1) while some acquired phenotypes of differentiated monocytes (region R2). As shown in Fig. 2*A*, STAT5A was constitutively phosphorylated on tyrosine residues in the MD1, MD2, and MD3 cells (*lanes 3-5*). The EMSA of these clones demonstrates that STAT5A in these cells showed DNA binding activity (Fig. 2*B*), which was supershifted by the anti-STAT5 Ab. Thus, STAT5A1*6 was constitutively activated in the retrovirally transduced M1 cells and induced differentiation of M1 cells into a macrophage lineage.

Constitutively active STAT5A induced tyrosine phosphorylation of STAT3 in M1 cells

Using the M1 stable transfectants expressing STAT5A1*6 (MD1–3), we attempted to clarify the molecular mechanism by which STAT5A1*6 induced macrophage differentiation of M1 cells. It was reported that a dominant-negative form of STAT3 profoundly inhibited IL-6-induced macrophage differentiation of M1 cells, and that STAT3 was likely to play a central role in the differentiation of M1 cells (23). In contrast, because IL-3 and GM-CSF are capable of inducing granulocyte-macrophage colony formation in in vitro cultures of bone marrow cells of normal mice (24), STAT5 may also play a role in myelomonocytic development. We first asked whether STAT3 in MD cells was phosphorylated on tyrosine residues. Indeed, STAT3 was phosphorylated on tyrosine residues in MD cells expressing STAT5A1*6 (Fig. 3*A*, *lanes 3-5*), but not in parental M1 cells or M1 cells expressing the wild-type STAT5A (Fig. 3*A*, *lanes 1* and *2*). One possibility was that the constitutively active STAT5A heterodimerized with STAT3. To test the possible interaction between STAT5A1*6 and STAT3 in MD cells, we performed immunoprecipitation using the anti-STAT5A Ab followed by immumoblotting with the anti-STAT3 Ab and vice versa. However, we did not detect a heterodimer of STAT5 and STAT3 in MD cells (Fig. 3*B*), indicating that STAT5A1*6 was capable of inducing activation of STAT3 through mechanisms other than forming heterodimers with STAT3.

The constitutively active STAT5A induced production of IL-6

It was reported that IL-3 induced production of IL-6 in several IL-3-dependent hemopoietic cells (25). Because STAT5A is one of the key molecules that mediate IL-3-induced cell signaling (26),

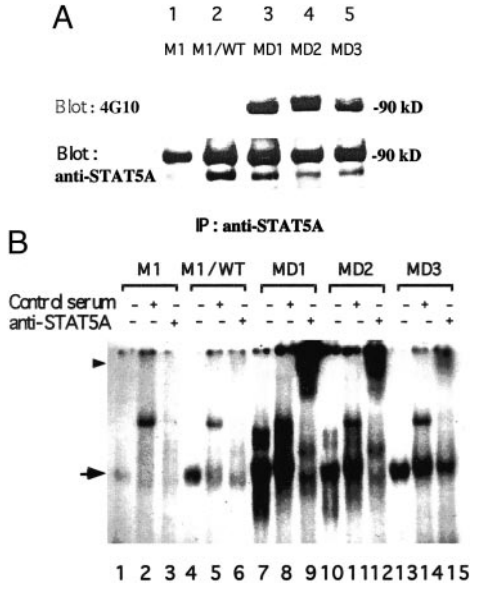

FIGURE 2. Characterization of the STAT5A1*6 expressed in MD cells. *A*, Tyrosine phosphorylation of STAT5A in parental M1, M1/WT-STAT5A, and MD cells. Cells were lysed, and STAT5A proteins were immunoprecipitated with the anti-STAT5A Ab. The immunoprecipitated proteins were separated by a SDS-polyacrylamide gradient gel and analyzed by Western blot with the anti-phosphotyrosine Ab (*upper panel*), followed by probing with the anti-STAT5A Ab (*lower panel*). *B*, DNA binding activities of STAT5A in nuclear extracts derived from parental M1, M1/WT-STAT5A, and MD1–3 cells. The DNA-protein complexes were confirmed to contain STAT5A by supershift analysis using anti-STAT5A Ab. An arrowhead and an arrow indicate positions of the STAT5A bands and supershifted complexes, respectively.

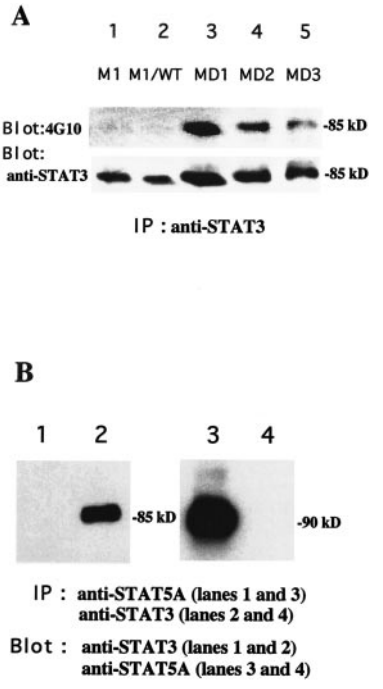

FIGURE 3. Analysis of STAT3 in MD1–3 cells. *A*, Tyrosine phospholylation of STAT3 in parental M1, M1/WT-STAT5A, and MD cells. Cells were treated as described for Fig. 2*A*. An anti-STAT3 Ab was used here instead of anti-STAT5A Ab. *B*, Failure to detect heterodimers of STAT3 and STAT5A1*6. Bulk population of MD cells was lysed and STAT3 and STAT5A proteins were immunoprecipitated with anti-STAT3 (*lanes 1* and *3*) and anti-STAT5A (*lanes 2* and *4*) Abs, respectively. The immunoprecipitated proteins were subjected to SDS-PAGE analysis using a gradient gel and analyzed by Western blot with anti-STAT3 (*lanes 1* and *2*) and anti-STAT5A Abs (*lanes 3* and *4*).

and IL-6 induces STAT3 activation through IL-6R (27–29), we hypothesized that STAT5A1*6 induces macrophage differentiation of M1 cells through activation of IL-6 production. To test this hypothesis, we examined the supernatant of MD cells for the ability to induce differentiation of parental M1 cells. As shown in Fig. 4*A*, the supernatant of the MD cells induced macrophage differentiation in parental M1 cells, and an anti-IL-6 neutralizing Ab (10 μg/ml) profoundly blocked this activity of the supernatant. The anti-IL-6 neutralizing Ab (10 μg/ml) also led to decreased tyrosine phosphorylation of STAT3 in parental M1 cells (Fig. 4*B*). In addition, IL-6 mRNA was readily detected in the MD cells, but not so in parental M1 cells (Fig. 4*C*). Thus, STAT5A1*6 expressed in MD cells produced a sufficient amount of IL-6 production to induce macrophage differentiation of parental M1 cells via activation of STAT3.

Mechanisms by which MD cells escaped apoptosis after terminal differentiation induced by autocrined IL-6

Whereas the supernatant of the MD cells strongly induced terminal differentiation and eventually apoptosis in parental M1 cells, the MD cells proliferated continuously, with some populations having differentiated phenotypes. To identify key molecules that inhibited MD cells from apoptosis following terminal differentiation in the supernatant containing high concentrations of IL-6, we generated a cDNA library in a retrovirus vector pMXneo (30) from one of the MD clones, MD1. Genes with the potential to inhibit apoptosis following terminal differentiation were searched for in retrovirus-mediated functional screening of the MD-1-derived cDNA library; M1 cells infected with the cDNA library were screened for clones resistant to IL-6-induced apoptosis in a medium containing IL-6 (100 ng/ml) and G418 selection reagents (600 μg/ml). A clone that survived and grew in the presence of IL-6 was isolated after screening of 1.5×10^5 independent cDNA clones. The integrated cDNA in the clone, recovered by PCR with vector primers, was sequenced. The cDNA integrated in the clone was found to be a sense cDNA encoding the full-length of A1, which is a member of the *bcl-2* family of proteins known to inhibit apoptosis (31–33). As shown in Fig. 5*A*, the expression level of *A1* mRNA was extremely high in MD cells, but undetectable in parental M1 cells. In addition, expression of *A1* mRNA was not detected when parental M1 cells underwent IL-6-induced terminal differentiation and apoptosis (data not shown), which suggested that *A1* was one of the responsible genes for the resistance of MD cells to IL-6-induced apoptosis following terminal differentiation. To confirm that expression of the *A1* gene protected M1 cells from IL-6-induced apoptosis, *A1* cDNA was subcloned into pMX-IRES-EGFP and reintroduced into M1 cells. As a control, pMX-IRES-EGFP was also introduced into M1 cells. EGFP-positive cells were sorted on FACS 48 h after virus infection, as described in *Materials and Methods*. Morphological changes of both M1 transfectants under the treatment with IL-6 (10 ng/ml) for 5 days are shown in Fig. 5*B*. Consistent with an observation previously reported (31), the constitutive expression of *A1* efficiently protected M1 cells from IL-6-induced apoptosis. Therefore, STAT5A1*6 induced not only IL-6 production that could induce macrophage differentiation of parental M1 cells, but also expression of *A1* that could counterbalance the effect of IL-6 by protecting M1 cells from apoptosis following terminal differentiation.

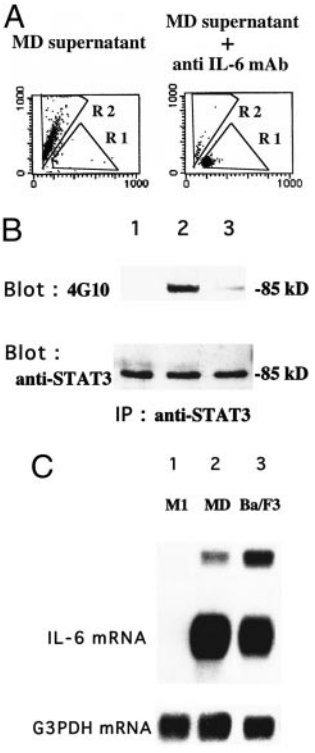

FIGURE 4. The supernatant of MD cells contains a sufficient amount of IL-6 to induce macrophage differentiation of parental M1 cells via activation of STAT3. *A*, Parental M1 cells were cultured in the medium containing half-volume of the supernatant of the MD1 cells with (*right panel*) or without (*left panel*) an anti-IL-6 neutralizing Ab (10 μg/ml). Flow cytometric analysis was performed to quantitate the morphological changes in these cells 3 days after the treatment. Differentiated M1 cells were detected in region R2. Increased size and vacuolization of differentiated cells are reflected by increases in FSC (*x*-axis) and SSC (*y*-axis), respectively. MD2 and MD3 cells gave similar results (data not shown). *B*, Tyrosine phosphorylation of STAT3 in parental M1 (*lane 1*) and M1 cells incubated in the supernatant of MD cells for 30 min with (*lane 3*) or without (*lane 2*) the anti-IL-6 neutralizing Ab (10 μg/ml). Cells were treated as described for Fig. 3*A*. *C*, Expression of IL-6 mRNA in parental M1, MD, and Ba/F3 cells cultured in medium containing IL-3 (1 ng/ml) as a positive control. A total of 2 μg poly(A)$^+$ RNA was subjected to Northern blot analysis. A full-length cDNA for mIL-6 was used as a probe.

*An anti-IL-6 neutralizing Ab profoundly blocked macrophage differentiation of M1 cells induced by STAT5A1*6*

To confirm that the autocrined IL-6 played a central role in STAT5A1*6-induced macrophage differentiation of M1 cells, we cultured the STAT5A1*6-transduced M1 cells in the presence of an anti-mIL-6 neutralizing Ab (10 μg/ml) immediately after the sorting of EGFP-positive cells. The anti-IL-6 Ab profoundly inhibited the differentiation of M1 cells expressing STAT5A1*6 (Fig. 6). We also confirmed that an isotype control Ab did not affect this differentiation (data not shown). These results clearly show that STAT5A1*6 induced differentiation of M1 cells through autocrine production of IL-6.

The promoter of IL-6 is transactivated by activation of STAT5A through enhanced DNA binding activity of NF-κB p65

Next, we asked whether STAT5A directly activated the promoter of the IL-6 gene, which does not contain the typical STAT5A binding site (34). For this, we did a transactivation assay in which Ba/F3 cells were cotransfected with IL-6 promoter-luciferase reporter constructs harboring various deletions in the IL-6 promoter

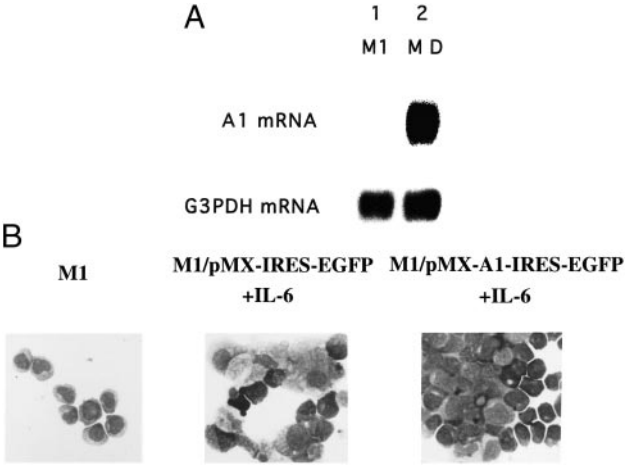

FIGURE 5. A1 expression prevented M1 cells from IL-6-induced terminal differentiation. *A*, A1 gene expression was detected by Northern blot analysis in MD cells (*lane 2*) but not in parental M1 cells (*lane 1*). *B*, Morphological analysis of M1 cells expressing A1 treated with IL-6 (10 ng/ml).

region (Fig. 7*A*), and a vector carrying the wild-type STAT5A or STAT5A1*6. As shown in Fig. 7*B*, the transactivating activity of pMX-STAT5A1*6 toward the wild-type IL-6 promoter (k0) was stronger (~30-fold) than that of pMX-STAT5A in the absence of IL-3. Using mutant constructs, mk9 and mk0, harboring mutations

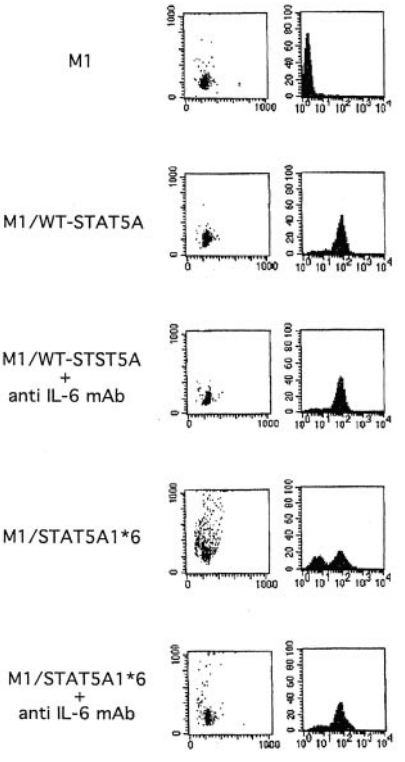

FIGURE 6. Inhibition of macrophage differentiation in M1/STAT5A1*6 cells with an anti-mIL-6 neutralizing Ab. M1 cells were retrovirally transduced with pMX-STAT5A1*6-IRES-EGFP, and EGFP-positive cells were sorted on a cell sorter 2 days after gene transduction. pMX-STAT5A-IRES-EGFP served as a control vector. M1/STAT5A1*6 cells were then separated and cultured under different conditions: half were cultured in the medium with an anti-IL-6 Ab (10 μg/ml), and the other half were cultured with a control Ab (10 μg/ml). Quantitation of M1 cell differentiation and expression of EGFP were analyzed on FACS.

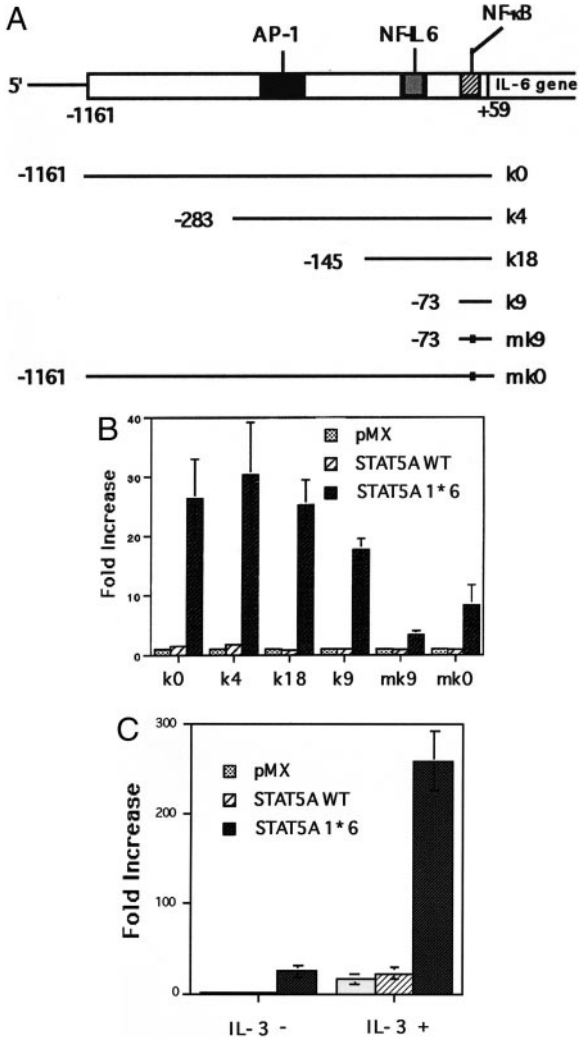

FIGURE 7. Transactivation of the wild-type IL-6 promoter and its mutants by STAT5A. *A*, The structures of the wild-type and various mutants of the IL-6 promoter. The wild-type IL-6 promoter sequence, k0 (−1161/+59), contains AP-1 (−283/−277), NF-IL-6 (−145/−158), and NF-κB (−73/−64) binding sites. The deletion mutants were designed as k4 (−310/+59), k18 (−180/+59), and k9 (−122/+59). The mk9 and mk0 was produced by introducing a mutation in the NF-κB binding site of the k9 and k0 to reduce the NF-κB binding activity, as described in *Materials and Methods*. *B*, The sequence for luciferase was connected up with the wild-type IL-6 promoter (k0) or the various mutants of the IL-6 promoter (k4, k18, k9, mk9, and mk0) in reporter plasmids. Luciferase activities were examined in the lysates of Ba/F3 cells cotransfected with each of these reporter plasmids and either of the mock vector (pMX), the expression vector for the wild-type STAT5A (pMX/STAT5A-WT), or that for the STAT5A1*6 (pMX/STAT5A1*6), as described in *Materials and Methods*. The results shown are the averages ± SD of three independent experiments. *C*, Transactivation of the wild-type IL-6 promoter (k0) by the wild-type STAT5A and STAT5A1*6 in the presence of IL-3. Luciferase activities were examined in the lysates of Ba/F3 cells cotransfected with the k0 reporter plasmids and either of the mock vector (pMX), the expression vector for the wild-type STAT5A (pMX/STAT5A-WT), or that for the STAT5A1*6 (pMX/STAT5A1*6), as described in *Materials and Methods*. Cells were stimulated with 1 ng/ml of mIL-3 for the last 6 h before cell lysates were prepared. The results shown are the averages ± SD of three independent experiments.

in the NF-κB binding site, it was also found that the NF-κB binding site was indispensable in the STAT5A-induced transactivation of the IL-6 promoter. When Ba/F3 cells were treated with IL-3 (1 ng/ml) after cotransfection with k0, the transactivating activities of both pMX-STAT5A and pMX-STAT5A1*6 were more potent (~10-fold) than those without IL-3 treatment (Fig. 7*C*). These results are consistent with our previous data describing the transactivation potency of STAT5A1*6 (8). We also reported that another STAT5A mutant, STAT5A-N642H, harboring a point mutation in the Src homology 2 domain showed a phenotype identical with that of STAT5A1*6 (9), indicating that the finding with STAT5A1*6 was not unique to a particular mutant. These data suggest that activation of STAT5A by IL-3 induced transactivation of the IL-6 promoter through the NF-κB binding site.

To see whether NF-κB activation is involved in the STAT5A-mediated transactivation of IL-6, we performed EMSA using COS cells after transient gene expression of EpoR and STAT5A, as described in *Materials and Methods*. As shown in Fig. 8, the DNA binding activity of NF-κB p65 in cells cotransfected with pMX-STAT5A1*6 (*lane 5*) was notably enhanced compared with those in cells cotransfected with pMX and pMX-STAT5A (*lanes 3* and *4*). When COS cells were stimulated with Epo after cotransfection, the DNA binding activities of NF-κB p65 in the cells were also enhanced (*lanes 2*, *4*, and *6*) compared with those without treatment of Epo (*lanes 1*, *3*, and *5*). The DNA-protein complexes were confirmed to contain NF-κB p65, but not STAT5A, using an anti-NF-κB p65 Ab (*lanes 7–12*) or an anti-STAT5A Ab (data not shown). The DNA binding activity of NF-κB p50 was not affected by the coexpression of STAT5A without stimulation (data not shown).

We also conducted EMSA to analyze the DNA binding activities of NF-κB in M1/WT-STAT5A and MD cells expressing the constitutively active STAT5 mutant STAT5A1*6. As shown in Fig. 9*A*, the DNA-protein complex formation was specific to the oligonucleotides corresponding to the NF-κB site and enhanced in MD cells. In addition, the DNA-protein complexes in MD cells showed a slower mobility than those in M1/WT-STAT5A cells. These results suggest that the DNA-NF-κB complexes in MD cells were somehow modulated by STAT5A1*6 and formed larger complexes that may contain additional molecule(s). Using the anti-NF-κB p65 Ab, we found that the lower band of the DNA-NF-κB complexes contained NF-κB p65 (Fig. 9*B*). In contrast, the upper band of the DNA-protein complexes in MD cells contained c-Rel (Fig. 9*C*). These findings imply that activation of STAT5A transactivated IL-6 expression not only by enhancing the DNA binding

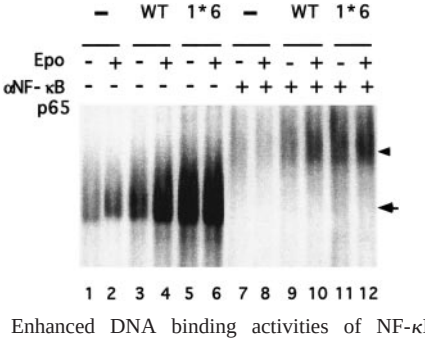

FIGURE 8. Enhanced DNA binding activities of NF-κB p65 by STAT5A activation. DNA binding activities of NF-κB p65 were examined by EMSA using nuclear extracts derived from COS cells expressing the Epo receptor and either the wild-type STAT5A (WT), the STAT5A1*6 (1*6), or the control vector pMX (−), with or without Epo stimulation. The DNA-protein complexes were confirmed to contain NF-κB p65 in a supershift analysis with an anti-NF-κB p65 Ab. The arrowhead and arrow indicate positions of the DNA-NF-κB p65 complexes and supershifted complexes, respectively.

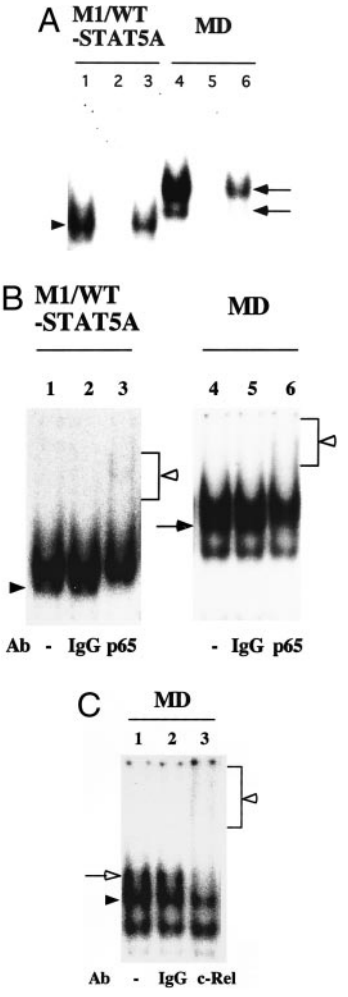

FIGURE 9. Enhanced DNA binding activities of NF-κB p65 and c-Rel and modulation of DNA-protein complexes of NF-κB p65 by STAT5A activation in MD cells. *A*, Nuclear extracts of M1/WT-STAT5A (*lanes 1–3*) and MD cells (*lanes 4–6*) were prepared and subjected to EMSA with ^{32}P-labeled oligonucleotide probe containing an NF-κB binding sequence. Competition assays were performed by adding 5-fold molar excess of cold competitor (*lanes 2* and *5*) or nonspecific oligonucleotides (*lanes 3* and *6*) in the reaction mixture. The arrowhead indicates the specific DNA-protein complexes, and arrows indicate STAT5A1*6-induced supershifted complexes. *B*, DNA binding activities of NF-κB p65 were examined by EMSA using nuclear extracts derived from M1/WT-STAT5A (*lanes 1–3*) and MD cells (*lanes 4–6*). The filled arrowhead and arrow indicate positions of the DNA-NF-κB p65 complexes in M1/WT-STAT5A cells and MD cells, respectively. The open arrowheads indicate positions of the supershifted bands. *C*, DNA binding activities of c-Rel were examined by EMSA using nuclear extracts derived from MD cells. The open arrow and the open arrowhead indicate positions of the DNA-c-Rel complexes and supershifted bands, respectively. The filled arrowhead indicates positions of the DNA-NF-κB p65 complexes.

activity of NF-κB p65 and c-Rel, but also by modulating the DNA-protein complexes of NF-κB p65 in MD cells. Using the anti-STAT5A Ab, we also performed EMSA in MD cells to test whether this mobility shift was induced by the direct association of STAT5A1*6 with the DNA-NF-κB complexes. However, the DNA-NF-κB complexes were not supershifted by the anti-STAT5A Ab (data not shown). We are now investigating how expression of STAT5A1*6 leads to mobility shift of the DNA-protein complexes of NF-κB p65 in MD cells.

Discussion

We previously demonstrated pleiotropic functions of STAT5 in a model system using a mIL-3-dependent pro-B cell line, Ba/F3, in which STAT5 activation induced proliferation, macrophage differentiation, and apoptosis through induction of *pim-1*, $p21^{WAF/Cip1}$, and *suppressor of cytokine signaling-1/STAT-induced STAT inhibitor-1/Janus kinase binding protein*, respectively. In the present work, we found that a constitutively active mutant of STAT5A (STAT5A1*6) induced monocyte/macrophage differentiation of a murine myeloblastic leukemia cell line, M1, through a distinct mechanism, autocrine production of IL-6 in M1 cells. Interestingly, STAT5 seemed to collaborate with NF-κB p65 in inducing IL-6 production in M1 cells.

We first considered that $p21^{WAF/Cip1}$ played important roles in inducing M1 differentiation because $p21^{WAF/Cip1}$ was a target gene of STAT5 (25, 35, 36). In fact, overexpression of $p21^{WAF/Cip1}$ alone was able to induce partial differentiation of Ba/F3 cells into macrophage-like cells (10). However, this was not the case in MD cells; STAT5A1*6 did not induce detectable levels of $p21^{WAF/Cip1}$ (data not shown). Instead, we found that STAT5A1*6 transactivated the IL-6 promoter, and that produced IL-6-induced STAT3 activation and macrophage differentiation in an autocrine fashion. It is known that transactivation of the IL-6 promoter is regulated by NF-κB, NF-IL-6, and AP-1 (37, 38), and that the promoter region contains no STAT5 binding sites. Using deletion mutants of the IL-6 promoter, we found that the NF-κB binding site of the IL-6 promoter was sufficient for STAT5A-induced transactivation of IL-6. Moreover, the DNA binding activity of NF-κB p65 was enhanced by STAT5A1*6. These results indicate that the STAT5A-induced IL-6 production was mediated by NF-κB activation. This was analogous to the reported data that STAT6 and NF-κB are directly associated and function in a synergistic fashion (39). However, we were not able to demonstrate direct interaction between STAT5 and NF-κB p65 (data not shown). It is possible that other transcription factors, such as CREB binding protein/p300 or a protein induced by STAT5, mediate their interaction. In addition to IL-6, LIF and OSM, other members of the IL-6 family cytokines, are also produced from Ba/F3 cells in response to IL-3 stimulation, and the promoter region of OSM actually harbors STAT5 binding sites (36). These data suggest that OSM is the ancestral gene of the IL-6 gene family, and that production of these three cytokines is regulated essentially by the same mechanism, although the promoter of OSM, but not those of IL-6 and LIF, carries the STAT5 binding sites.

Our findings provide evidence for a novel capability of STAT5 to cooperate with NF-κB p65 in inducing production of IL-6, and this notion is consistent with several observations reported by other investigators. First, in a patient with follicular lymphoma, autologous bone marrow transplantation with high-dose IL-3 treatment induced terminal differentiation of the lymphoma cells into plasma cells followed by a long-lasting remission. This phenomenon was preceded by elevation of the serum level of IL-6 after the treatment with IL-3 (40). Second, the roles of NF-κB in macrophage differentiation have been reported (41–43). Activation of IL-6 gene expression through NF-κB and the roles of IL-6 in macrophage differentiation were also reported (14, 37, 38). Finally, GM-CSF induces NF-κB activation in some types of hemopoietic cells (44, 45). We also found that IL-3 induced NF-κB transactivation in a reporter assay in Ba/F3 cells (Fig. 7*C*). Therefore, we propose a novel signal cascade of myelomonocytic development: IL-3 and/or GM-CSF→STAT5→NF-κB→IL-6 autocrine→macrophage differentiation.

Analysis of c-*rel*$^{-/-}$ mice revealed that Rel/NF-κB is a critical transactivator of the promoter of the *A1* gene (46). Although the promoter of *A1* does not contain the typical STAT5A binding site (46), STAT5A1*6 strongly induced *A1* expression in M1 cells (Fig. 5*B*). As shown in Fig. 9*C*, STAT5A1*6 apparently enhanced the DNA binding activity of c-Rel as well as NF-κB p65. Therefore, it is likely that STAT5A1*6 controlled expression of the *A1* gene as well as the *IL-6* gene via enhanced binding of Rel/NF-κB to the promoters. An antiapoptotic activity of STAT5 in primary myeloid hemopoietic cells has also been reported by Kieslinger et al. (47). They demonstrated antiapoptotic activity of STAT5 through the *bcl-2* family gene, *bcl-x*, whose promoter contains binding sites of STAT5.

In addition to the promoter of IL-6, STAT5A1*6 transactivated the HIV promoter, which has the NF-κB site but not STAT5 binding sites (48) (T. Kawashima and T. Kitamura, unpublished results). Thus, cooperation of STAT5 and NF-κB may play a role in manifesting pleiotropic functions of STAT5.

The finding that STAT5A activation stimulates autocrine production of IL-6 implies an interesting possibility that downstream signals of the IL-3 or the GM-CSF receptor by themselves may not be sufficient to stimulate terminal differentiation of hemopoietic progenitors. Additional signals mediated by autocrine cytokines, such as IL-6 induced by IL-3 and GM-CSF, may be required for terminal differentiation of progenitor cells into myelomonocytic lineages.

Acknowledgments

We thank T. A. Takahashi and T. Nakahata for FACS machines, A. Kaneko for excellent sorting on FACS, and M. Ohara for language assistance.

References

1. Wakao, H., F. Gouilleux, and B. Groner. 1995. Mammary gland factor (MGF) is a novel member of the cytokine regulated transcription factor gene family and confers the prolactin response. *EMBO J. 14:854.*
2. Wakao, H., N. Harada, T. Kitamura, A. L. Mui, and A. Miyajima. 1995. Interleukin-2 and erythropoietin activate STAT5/MGF via distinct pathways. *EMBO J. 14:2527.*
3. Azam, M., H. Erdjument-Bromage, B. L. Kreider, M. Xia, F. Quelle, R. Basu, C. Saris, P. Tempst, J. N. Ihle, and C. Schindler. 1995. Interleukin-3 signals through multiple isoforms of Stat5. *EMBO J. 14:1402.*
4. Fujii, H., Y. Nakagawa, U. Schindler, A. Kawahara, H. Mori, F. Gouilleux, B. Groner, J. N. Ihle, Y. Minami, T. Miyazaki, et al. 1995. Activation of Stat5 by interleukin 2 requires a carboxyl-terminal region of the interleukin 2 receptor β chain but is not essential for the proliferative signal transmission. *Proc. Natl. Acad. Sci. USA 92:5482.*
5. Miyakawa, Y., A. Oda, B. J. Druker, H. Miyazaki, M. Handa, H. Ohashi, and Y. Ikeda. 1996. Thrombopoietin induces tyrosine phosphorylation of Stat3 and Stat5 in human blood platelets. *Blood 87:439.*
6. Mui, A. L., H. Wakao, A. M. O'Farrell, N. Harada, and A. Miyajima. 1995. Interleukin-3, granulocyte-macrophage colony stimulating factor and interleukin-5 transduce signals through two STAT5 homologs. *EMBO J. 14:1166.*
7. Pallard, C., F. Gouilleux, L. Benit, L. Cocault, M. Souyri, D. Levy, B. Groner, S. Gisselbrecht, and I. Dusanter-Fourt. 1995. Thrombopoietin activates a STAT5-like factor in hematopoietic cells. *EMBO J. 14:2847.*
8. Onishi, M., T. Nosaka, K. Misawa, A. L. Mui, D. Gorman, M. McMahon, A. Miyajima, and T. Kitamura. 1998. Identification and characterization of a constitutively active STAT5 mutant that promotes cell proliferation. *Mol. Cell. Biol. 18:3871.*
9. Ariyoshi, K., T. Nosaka, K. Yamada, M. Onishi, Y. Oka, A. Miyajima, and T. Kitamura. 2000. Constitutive activation of STAT5A by a point mutation in the SH2 domain. *J. Biol. Chem. 275:24407.*
10. Nosaka, T., T. Kawashima, K. Misawa, K. Ikuta, A. L. Mui, and T. Kitamura. 1999. STAT5 as a molecular regulator of proliferation, differentiation and apoptosis in hematopoietic cells. *EMBO J. 18:4754.*
11. Ichikawa, Y. 1969. Differentiation of a cell line of myeloid leukemia. *J. Cell. Physiol. 74:223.*
12. Selvakumaran, M., D. Liebermann, and B. Hoffman-Liebermann. 1993. Myeloblastic leukemia cells conditionally blocked by *myc*-estrogen receptor chimeric transgenes for terminal differentiation coupled to growth arrest and apoptosis. *Blood 81:2257.*
13. Bruce, A. G., I. H. Hoggatt, and T. M. Rose. 1992. Oncostatin M is a differentiation factor for myeloid leukemia cells. *J. Immunol. 149:1271.*
14. Shabo, Y., J. Lotem, M. Rubinstein, M. Revel, S. C. Clark, S. F. Wolf, R. Kamen, and L. Sachs. 1988. The myeloid blood cell differentiation-inducing protein MGI-2A is interleukin-6. *Blood 72:2070.*
15. Gearing, D. P., N. M. Gough, J. A. King, D. J. Hilton, N. A. Nicola, R. J. Simpson, E. C. Nice, A. Kelso, and D. Metcalf. 1987. Molecular cloning and expression of cDNA encoding a murine myeloid leukaemia inhibitory factor (LIF). *EMBO J. 6:3995.*
16. Smith, A., D. Metcalf, and N. A. Nicola. 1997. Cytoplasmic domains of the common β-chain of the GM-CSF/IL-3/IL-5 receptors that are required for inducing differentiation or clonal suppression in myeloid leukaemic cell lines. *EMBO J. 16:451.*
17. Miyajima, A., A. L. Mui, T. Ogorochi, and K. Sakamaki. 1993. Receptors for granulocyte-macrophage colony-stimulating factor, interleukin-3, and interleukin-5. *Blood 82:1960.*
18. Miyajima, A., J. Schreurs, K. Otsu, A. Kondo, K. Arai, and S. Maeda. 1987. Use of the silkworm, *Bombyx mori*, and an insect baculovirus vector for high-level expression and secretion of biologically active mouse interleukin-3. *Gene 58:273.*
19. Pear, W. S., G. P. Nolan, M. L. Scott, and D. Baltimore. 1993. Production of high-titer helper-free retroviruses by transient transfection. *Proc. Natl. Acad. Sci. USA 90:8392.*
20. Kitamura, T., M. Onishi, S. Kinoshita, A. Shibuya, A. Miyajima, and G. P. Nolan. 1995. Efficient screening of retroviral cDNA expression libraries. *Proc. Natl. Acad. Sci. USA 92:9146.*
21. Okumura, N., K. Tsuji, Y. Ebihara, I. Tanaka, N. Sawai, K. Koike, A. Komiyama, and T. Nakahata. 1996. Chemotactic and chemokinetic activities of stem cell factor on murine hematopoietic progenitor cells. *Blood 87:4100.*
22. Isshiki, H., S. Akira, O. Tanabe, T. Nakajima, T. Shimamoto, T. Hirano, and T. Kishimoto. 1990. Constitutive and interleukin-1 (IL-1)-inducible factors interact with the IL-1-responsive element in the IL-6 gene. *Mol. Cell. Biol. 10: 2757.*
23. Nakajima, K., Y. Yamanaka, K. Nakae, H. Kojima, M. Ichiba, N. Kiuchi, T. Kitaoka, T. Fukada, M. Hibi, and T. Hirano. 1996. A central role for Stat3 in IL-6-induced regulation of growth and differentiation in M1 leukemia cells. *EMBO J. 15:3651.*
24. Prystowsky, M. B., G. Otten, M. F. Naujokas, J. Vardiman, J. N. Ihle, E. Goldwasser, and F. W. Fitch. 1984. Multiple hemopoietic lineages are found after stimulation of mouse bone marrow precursor cells with interleukin 3. *Am. J. Pathol. 117:171.*
25. Yoshimura, A., M. Ichihara, I. Kinjyo, M. Moriyama, N. G. Copeland, D. J. Gilbert, N. A. Jenkins, T. Hara, and A. Miyajima. 1996. Mouse oncostatin M: an immediate early gene induced by multiple cytokines through the JAK-STAT5 pathway. *EMBO J. 15:1055.*
26. Mui, A. L., H. Wakao, T. Kinoshita, T. Kitamura, and A. Miyajima. 1996. Suppression of interleukin-3-induced gene expression by a C-terminal truncated Stat5: role of Stat5 in proliferation. *EMBO J. 15:2425.*
27. Akira, S., Y. Nishio, M. Inoue, X. J. Wang, S. Wei, T. Matsusaka, K. Yoshida, T. Sudo, M. Naruto, and T. Kishimoto. 1994. Molecular cloning of APRF, a novel IFN-stimulated gene factor 3 p91-related transcription factor involved in the gp130-mediated signaling pathway. *Cell 77:63.*
28. Zhong, Z., Z. Wen, and J. E. Darnell, Jr. 1994. Stat3: a STAT family member activated by tyrosine phosphorylation in response to epidermal growth factor and interleukin-6. *Science 264:95.*
29. Yamanaka, Y., K. Nakajima, T. Fukada, M. Hibi, and T. Hirano. 1996. Differentiation and growth arrest signals are generated through the cytoplasmic region of gp130 that is essential for Stat3 activation. *EMBO J. 15:1557.*
30. Kawakami, Y., T. Miura, R. Bissonnette, D. Hata, W. N. Khan, T. Kitamura, M. Maeda-Yamamoto, S. E. Hartman, L. Yao, F. W. Alt, and T. Kawakami. 1997. Bruton's tyrosine kinase regulates apoptosis and JNK/SAPK kinase activity. *Proc. Natl. Acad. Sci. USA 94:3938.*
31. Lin, E. Y., A. Orlofsky, H. G. Wang, J. C. Reed, and M. B. Prystowsky. 1996. A1, a Bcl-2 family member, prolongs cell survival and permits myeloid differentiation. *Blood 87:983.*
32. Adams, J. M., and S. Cory. 1998. The Bcl-2 protein family: arbiters of cell survival. *Science 281:1322.*
33. Zong, W. X., L. C. Edelstein, C. Chen, J. Bash, and C. Gelinas. 1999. The prosurvival Bcl-2 homolog Bfl-1/A1 is a direct transcriptional target of NF-κB that blocks TNFα-induced apoptosis. *Genes Dev. 13:382.*
34. Ray, A., S. B. Tatter, L. T. May, and P. B. Sehgal. 1988. Activation of the human "β2-interferon/hepatocyte-stimulating factor/interleukin 6" promoter by cytokines, viruses, and second messenger agonists. *Proc. Natl. Acad. Sci. USA 85: 6701.*
35. el-Deiry, W. S., T. Tokino, V. E. Velculescu, D. B. Levy, R. Parsons, J. M. Trent, D. Lin, W. E. Mercer, K. W. Kinzler, and B. Vogelstein. 1993. WAF1, a potential mediator of p53 tumor suppression. *Cell 75:817.*
36. Harper, J. W., G. R. Adami, N. Wei, K. Keyomarsi, and S. J. Elledge. 1993. The p21 Cdk-interacting protein Cip1 is a potent inhibitor of G_1 cyclin-dependent kinases. *Cell 75:805.*
37. Libermann, T. A., and D. Baltimore. 1990. Activation of interleukin-6 gene expression through the NF-κB transcription factor. *Mol. Cell. Biol. 10:2327.*
38. Matsusaka, T., K. Fujikawa, Y. Nishio, N. Mukaida, K. Matsushima, T. Kishimoto, and S. Akira. 1993. Transcription factors NF-IL-6 and NF-κB synergistically activate transcription of the inflammatory cytokines, interleukin 6 and interleukin 8. *Proc. Natl. Acad. Sci. USA 90:10193.*

39. Shen, C. H., and J. Stavnezer. 1998. Interaction of stat6 and NF-κB: direct association and synergistic activation of interleukin-4-induced transcription. *Mol. Cell. Biol. 18:3395.*
40. Kramer, M. H., P. M. Kluin, E. R. Wijburg, W. E. Fibbe, and H. C. Kluin-Nelemans. 1995. Differentiation of follicular lymphoma cells after autologous bone marrow transplantation and haematopoietic growth factor treatment. *Lancet 345:488.*
41. Ammon, C., K. Mondal, R. Andreesen, and S. W. Krause. 2000. Differential expression of the transcription factor NF-κB during human mononuclear phagocyte differentiation to macrophages and dendritic cells. *Biochem. Biophys. Res. Commun 268:99.*
42. Kurata, S., M. Matsumoto, and H. Nakajima. 1996. Transcriptional control of the heme oxygenase gene in mouse M1 cells during their TPA-induced differentiation into macrophages. *J. Cell. Biochem. 62:314.*
43. Conti, L., J. Hiscott, M. Papacchini, A. Roulston, M. A. Wainberg, F. Belardelli, and S. Gessani. 1997. Induction of relA (p65) and IκBα subunit expression during differentiation of human peripheral blood monocytes to macrophages. *Cell Growth. Differ. 8:435.*
44. Zhang, M.-Y., S.-C. Sun, L. Bell, and B. A. Miller. 1998. NF-κB transcription factors are involved in normal erythropoiesis. *Blood. 91:4136.*
45. Pyatt, D. W., W. S. Stillman, Y. Yang, S. Gross, J. H. Zheng, and R. D. Irons. 1999. An essential role for NF-κB in human $CD34^+$ bone marrow cell survival. *Blood. 93:3302.*
46. Grumont, R. J., I. J. Rourke, and S. Gerondakis. 1999. Rel-dependent induction of A1 transcription is required to protect B cells from antigen receptor ligation-induced apoptosis. *Genes Dev. 13:400.*
47. Kieslinger, M., I. Woldman, R. Moriggl, J, Hofmann, J. C. Marine, J. N. Ihle, H. Beug, and T. Decker. 2000. Antiapoptotic activity of Stat5 required during terminal stages of myeloid differentiation. *Genes Dev. 14:232.*
48. Nabel, G., and D. Baltimore. 1987. An inducible transcription factor activates expression of human immunodeficiency virus in T cells. [Published erratum appears in *1990 Nature 344:178.*] *Nature 326:711.*